

# New Aspects in the Calculation of Electronic Momentum Properties; an All-Quantum Study

Michael C. Böhm, Rafael Ramírez <sup>a</sup>, and Joachim Schulte\*

Institut für Physikalische Chemie, Physikalische Chemie III, Technische Universität Darmstadt, Petersenstr. 20, D-64287 Darmstadt

<sup>a</sup> Instituto de Ciencia de Materiales, Consejo Superior de Investigaciones Científicas, Cantoblanco, E-28049 Madrid

Z. Naturforsch. **53 a**, 38–44 (1998); received November 22, 1997

The electronic properties of the C<sub>6</sub>H<sub>6</sub> and C<sub>6</sub>D<sub>6</sub> molecules have been studied by an all-quantum approach, where the classical and quantum degrees of freedom of the nuclei are taken into account in the evaluation of electronic expectation values. In the all-quantum approach suggested a Feynman path integral Monte Carlo (PIMC) formalism has been linked to an electronic *ab initio* Hamiltonian. The electronic expectation values have been calculated as averages over the manifold of nuclear configurations populated in thermal equilibrium. This theoretical setup leads to electronic expectation values that depend on the temperature and on the mass of the nuclei. The ensemble averaged electronic properties differ sizeably from the results derived on the basis of a single nuclear configuration of minimum energy. This behaviour should have physical implications for the theoretical calculation of electronic momentum properties such as Compton profiles, reciprocal form factors, etc. We describe an error source in the theoretical determination of electronic momentum properties which has not been commented so far.

**Key words:** Quantum Properties of Nuclei and Electrons; Path-Integral Simulations; *ab initio* Calculations; Electronic Momentum Properties; Finite-Temperature and Isotope Effects.

## 1. Introduction

The momentum distribution of electrons can be measured by Compton spectroscopy [1,2]. This technique completes the information which is accessible via diffraction experiments, i.e. the electron density distribution in real-space. The Compton profile corresponds to a one-dimensional (1D) projection of the electronic momentum distribution. Integration over all momenta yields the electronic kinetic energy  $\bar{E}_{\text{kin}}$ . With the aid of the virial theorem the total electronic energy  $\bar{E}_{\text{tot}}$  is accessible as well. Compton spectroscopy has the large advantage that measured intensities are dominated by contributions from the valence electrons, while diffraction intensities are dominated by contributions from the core electrons.

Improvements in experimental resolution techniques and data processing in the past years have been the prerequisites to perform high-precision measurements of Compton profiles [3]. The experimental research has been accompanied by theoretical calculations of Compton profiles or their Fourier transforms, the so-called reciprocal form factors. The comparative analysis of experimental and theoretical data, however, has shown that even sufficiently saturated *ab initio* basis sets are unable to reproduce measured Compton profiles quantitatively [4–6]. The discrepancy between measurement and calculation exceeds the experimental uncertainty. It is somewhat surprising to read that computational techniques even fail to reproduce the Compton profile of the most simple binary compound, LiH, with only two valence electrons per formula unit [7, 8].

The discrepancies between experiment and theory have been explained via the neglect of electronic correlation effects [5]. The majority of solid state calculations of Compton profiles reported in the literature is of the single-determinantal type only. A second

\* Present address: Bruker Analytische Meßtechnik GmbH, Silberstreifen, D-76287 Rheinstetten

Reprint requests to Prof. Dr. M. C. Böhm, Fax: +49 6151 164347, E-mail: boehm@pc07.pc.chemie.tu-darmstadt.de.

0932-0784 / 98 / 0100-0038 \$ 06.00 © – Verlag der Zeitschrift für Naturforschung, D-72072 Tübingen



Dieses Werk wurde im Jahr 2013 vom Verlag Zeitschrift für Naturforschung in Zusammenarbeit mit der Max-Planck-Gesellschaft zur Förderung der Wissenschaften e.V. digitalisiert und unter folgender Lizenz veröffentlicht: Creative Commons Namensnennung-Keine Bearbeitung 3.0 Deutschland Lizenz.

Zum 01.01.2015 ist eine Anpassung der Lizenzbedingungen (Entfall der Creative Commons Lizenzbedingung „Keine Bearbeitung“) beabsichtigt, um eine Nachnutzung auch im Rahmen zukünftiger wissenschaftlicher Nutzungsformen zu ermöglichen.

This work has been digitalized and published in 2013 by Verlag Zeitschrift für Naturforschung in cooperation with the Max Planck Society for the Advancement of Science under a Creative Commons Attribution-NoDerivs 3.0 Germany License.

On 01.01.2015 it is planned to change the License Conditions (the removal of the Creative Commons License condition “no derivative works”). This is to allow reuse in the area of future scientific usage.

possible error source in computational studies has been mentioned in the literature, the neglect of the kinetic energy of the nuclei  $T'$  [9]. These nuclear kinetic energy effects, however, should be of minor importance only. But even the single-determinantal argument seems to be debatable. The Compton profile is a typical one-electron property. It is commonly accepted (and verified numerically) that such one-electron properties are reproduced with good accuracy by calculations of the Hartree-Fock (HF) type. These methods generate one-electron densities which are correct up to first order in perturbation. Such a first-order criterion is not fulfilled for the electronic energy as well as for any other quantity which is influenced by electronic pair correlations.

It is the purpose of the present contribution to draw attention to another error source in the calculation of electronic momentum properties which has not been recognized so far. We have picked up this problem in course of our combined Feynman path integral Monte Carlo (PIMC) - *ab initio* investigations of molecules [10, 11]. The combination of a PIMC formalism for the nuclear degrees of freedom of molecules with ensuing electronic calculations offers the possibility to take into account the quantum character of the nuclei in the evaluation of electronic expectation values. It is the common disadvantage of the large majority of electronic structure calculations that the nuclei are treated as space-fixed classical particles which form a rigid background of point charges. Neither their classical thermal degrees of freedom nor their quantum fluctuations are considered when calculating electronic expectation values. Measured electronic quantities, however, correspond to averages over all nuclear configurations populated in thermal equilibrium as long as the time of the measurement exceeds the period of the corresponding vibrational modes. The conceptual shortcomings of electronic structure calculations working with frozen nuclei can be detected in many experiments; only some will be mentioned here. These are the temperature ( $T$ ) dependence of nuclear magnetic and nuclear quadrupole resonance (NMR, NQR) frequencies or the vibrational fine-structure of UV-VIS and photoelectron (PE) spectra. In our recent all-quantum studies [10 - 12] we have derived electronic expectation values which correspond to averages over many nuclear configurations. In the framework of the Born-Oppenheimer approximation (BOA) [13] the nuclei are free to thermally populate – with proper statistical weights – the states

of the vibrational problem. In our all-quantum approaches the PIMC generated nuclear configurations have been used as input for electronic structure calculations. This all-quantum strategy, which goes beyond the conventional single-configurational approaches of molecular quantum chemistry, leads to electronic matrix elements that depend on the temperature and on the mass of the nuclei. We have observed large nuclear quantum effects (= zero-point vibrations) in molecular systems with light atoms [10 - 12]. They are the microscopical origin of sizeable differences between electronic expectation values derived for a single nuclear configuration (here the optimized geometry) and the corresponding ensemble averages. In the present work we discuss these ensemble effects with special reference to possible consequences for electronic momentum properties such as Compton profiles.

It is not the purpose of the following discussion to calculate Compton profiles in the framework of such an all-quantum description, but to analyze differences between electronic matrix elements of the single-configuration type and ensemble averages derived under the consideration of the quantum and thermal degrees of freedom of the nuclei. The prohibitive computational expense of the all-quantum description of many-atom-many-electron fermion systems has restricted our theoretical analysis to a molecular model compound. But we are convinced that the general findings, that can be extracted from our study, have a strong implication for solid state properties such as Compton profiles. The differences between the two sets of electronic quantities (i.e. single-configuration results versus ensemble averages) will be studied as a function of temperature and characteristic isotope masses. The benzene molecule  $C_6H_6$  and its hexadeuterated isotopomer  $C_6D_6$  have been chosen as model systems. In the present work, electronic quantities have been averaged over 6000 different nuclear configurations which are populated according to the rules of the canonical statistics. To describe the quantum and thermal properties of the  $C_6H_6$  and  $C_6D_6$  nuclei, the powerful PIMC formalism of statistical physics has been used [14 - 18]. The nuclear Hamiltonian contains a model potential  $V(R)$  for the interatomic interaction which has been described in [19]. In order to reproduce the experimental CC bondlength  $r_{CC}$  of benzene [20] we have changed the  $r_{CC}$  value adopted in [19] into  $r_{CC} = 139.7$  pm. All other parameters in the definition of  $V(R)$  correspond to the design of [19]. The PIMC formalism for the nuclear

degrees of freedom has been linked to an electronic *ab initio* Hamiltonian of the HF type. The basis set we have adopted is of 3-21 G quality. We have used the GAMESS program as electronic structure tool [21]. The benzene bondlengths optimized by  $V(R)$  and by the *ab initio* approach are close to the experimental values [20]. We have:  $r_{CC} = 139.7, 140.7, 138.5$  pm;  $r_{CH} = 108.4, 109.7, 107.6$  pm (experimental values,  $V(R)$ , 3-21 G basis set, respectively).

The organization of the present paper is as follows. The theoretical background of our combined quantum approach as well as the computational conditions are given concisely in Section 2. The influence of the quantum character of the  $C_6H_6$  and  $C_6D_6$  nuclei on bare electronic expectation values is discussed in Section 3. The article ends with a short resumé.

## 2. Theoretical Background and Computational Conditions

Let us first introduce the quantities considered in the theoretical analysis of Section 3. The modified model potential  $V(R)$  from [19] has been employed to derive the potential and kinetic energy  $V$  and  $T'$  of the nuclear problem and to generate nuclear configurations populated in thermal equilibrium.  $V(R)$  should reproduce the *ab initio* potential surface as quantitatively as possible; the corresponding *ab initio* potential surface is defined by the total energy  $E_{tot}$  of the electronic Hamiltonian. An optimized setup of the all-quantum approach would require the identity  $V(R) = E_{tot}$ . In practice one has to accept, however, that  $V(R)$  can be only an approximation to the *ab initio* potential surface, i. e.  $V(R) \approx E_{tot}$ . The approximations that are part of the present combined PIMC - *ab initio* implementation have been described in detail in [11].  $E_{tot}$  of the electronic Hamiltonian is defined by the electronic kinetic energy  $E_{kin}$ , the electron-electron and core-core repulsions  $E_{el}$  and  $E_{nuc}$ , and the electron-core attraction  $E_{el-nuc}$  ( $E_{tot} = E_{kin} + E_{el} + E_{nuc} + E_{el-nuc}$ ). The three last elements on the rhs. of the equation in parenthesis define the potential energy  $E_{pot}$  of the electronic Hamiltonian ( $E_{tot} = E_{kin} + E_{pot}$ ). The (approximate) identity between  $V(R)$  and  $E_{tot}$  demonstrates that the potential energy of the nuclear problem contains the electronic kinetic energy  $E_{kin}$ . We have used the abbreviations  $E_i$  to denote single-configuration values of the electronic Hamiltonian. The corresponding equilibrium configuration

has been generated by  $V(R)$ . The ensemble averaged quantities sampled over 6000 different nuclear configurations will be abbreviated by  $\bar{E}_i$ . The discussion of the numerical results can be simplified if we adopt ensemble averaged quantities  $\bar{E}_i^*$  which are defined with respect to the single-configuration values  $E_i$  as energy origin, i. e.  $\bar{E}_i^* = \bar{E}_i - E_i$ . In connection with electronic momentum properties,  $E_{kin}$  and  $\bar{E}_{kin}^*$  are of particular interest. Subsequently it will be emphasized that  $\bar{E}_{kin}^*$  values that differ sizeably from zero may be a non-negligible error source in the theoretical calculation of Compton profiles or other electronic momentum properties. All calculations of these quantities, that have been published up to now, are based on single-configuration data  $E_{kin}$ . Remember that we have anticipated the ensemble character of the quantities  $\bar{E}_{kin}$  and  $\bar{E}_{tot}$  at the beginning of the present article.

The theoretical background of the PIMC formalism has been described in [14 - 18]. Our recent statistical investigations can be found in [10 - 12, 22, 23]. The key step of the PIMC formalism is the mapping of the partition function  $Z$  of the original quantum system onto a classical one which can be calculated with the aid of classical simulation techniques. If the number of quantum beads  $N$  is made large enough, the quantum partition function  $Z$  as well as all quantities that are derived from  $Z$  can be evaluated with high accuracy. We have adopted the classical Metropolis approach [24] to derive the thermal properties of  $C_6H_6$  and  $C_6D_6$  within the PIMC formalism. In the subsequent discussion of ensemble averaged electronic expectation values, temperatures of 50 and 750 K have been considered. The low-temperature properties of both systems are largely determined by zero-point vibrations ( $v = 0$ ;  $v$  is the vibrational quantum number) [10, 11, 22, 23]. At 750 K some of the benzene modes are excited to  $v = 1$  [25]. To derive the thermal properties of  $C_6H_6$  and  $C_6D_6$  we have performed  $5 \times 10^4$  MC steps.  $2 \times 10^4$  quantum paths have been taken into account for the system equilibration. The number of time-slices  $N$  has been fixed to obey the relation  $NT = 3000$  K, a statistical convergence criterion which leads to computational results of good quality [11]. At  $T = 50$  K this setup generates an ensemble of  $3 \times 10^6$  different nuclear configurations. At 750 K the number of configurations is reduced to  $2 \times 10^5$ . The error bars in the *ab initio* calculations caused by the ensemble reduction to 6000 in the electronic structure approach have been commented in [26].



### 3. Results and Discussion

The sizeable nuclear quantum effects occurring in  $C_6H_6$  and  $C_6D_6$  can be extracted from Fig. 1 where we have displayed calculated delocalization parameters of the different nuclei as a function of  $T$ . In the present work we have adopted atomic delocalization parameters in units of a squared length parameter ( $\text{pm}^2$ ). The total atomic delocalization  $d_{\text{tot}}^2$  is the superposition of the classical thermal delocalization  $d_c^2$  and the quantum delocalization  $d_q^2$  ( $d_{\text{tot}}^2 = d_c^2 + d_q^2$ ). At zero-temperature one has  $d_{\text{tot}}^2 = d_q^2$ . Here the spatial uncertainty of the atoms is due to zero-point fluctuations only.  $d_{\text{tot}}^2$  at  $T = 0$  K defines the squared amplitude of the zero-point vibrations. The quantum delocalization  $d_q^2$  in Fig. 1 has been derived in two different computational degrees of sophistication. In addition to the rather elaborate PIMC simulations we have employed the simple harmonic oscillator (ho) model [11, 23]. This approximation leads to an analytical formula for  $d_q^2$  (and  $d_c^2$  as well) [17, 22, 23]. The large differences

Table 1. Energy fragmentation of the *ab initio* 3-21 G energy of  $C_6H_6$  and  $C_6D_6$  at 50 and 750 K.  $E_{\text{kin}}$  denotes the kinetic energy of the electrons,  $E_{\text{nuc}}$  the nuclear-nuclear repulsion,  $E_{\text{el}}$  the two-electron repulsion,  $E_{\text{el-nuc}}$  the electron-core attraction,  $E_{\text{pot}}$  the potential energy of the electrons and  $E_{\text{tot}}$  the total energy of the electronic Hamiltonian. Note that  $E_{\text{tot}}$  contains a non-electronic element ( $= E_{\text{nuc}}$ ), but not the kinetic energy of the nuclei  $T'$ . The first set of numbers is based on a single-configuration approach (min); the corresponding geometry has been optimized by the interaction potential  $V(R)$ . All other quantities have been derived as ensemble averages over 6000 different nuclear configurations populated in thermal equilibrium. The ensemble averaged quantities are denoted as  $\bar{E}_i$ . The ensemble averages  $\bar{E}_i^*$  in the table are defined with respect to the  $E_i$  as energy zero, i. e.  $\bar{E}_i^* = \bar{E}_i - E_i$ . Negative  $\bar{E}_i^*$  entries symbolize a stabilization of the corresponding quantity under the influence of the nuclear dynamics relative to the single-configuration value; vice versa for positive  $\bar{E}_i^*$  entries. All parameters are given in eV.

Kind $i$ of energy	Optimized via $V(R)$ $E_i$	$C_6H_6$ $T = 50$ K $\bar{E}_i^*$	$C_6D_6$ $T = 50$ K $\bar{E}_i^*$	$C_6H_6$ $T = 750$ K $\bar{E}_i^*$	$C_6D_6$ $T = 750$ K $\bar{E}_i^*$
kin	6216.948	-4.116	-3.527	-5.022	-4.416
nuc	5488.821	-27.449	-25.001	-35.066	-31.811
el	7530.701	-28.487	-25.861	-36.410	-32.818
el-nuc	-25478.893	61.610	55.704	78.559	70.983
pot	-12459.371	5.674	4.842	7.143	6.354
tot	-6242.523	1.558	1.316	2.121	1.938

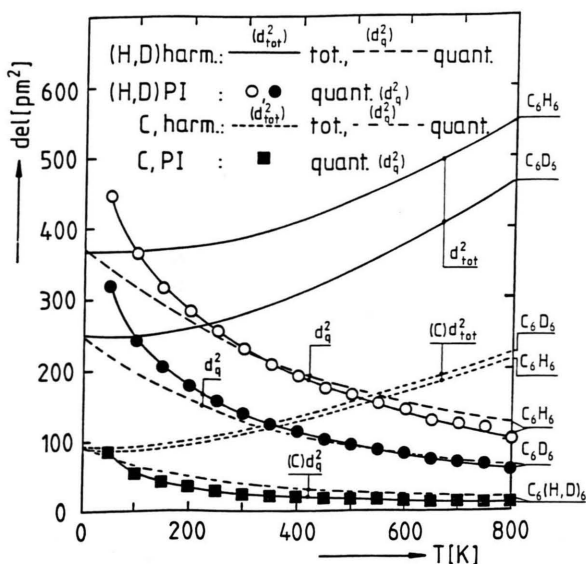


Fig. 1. Atomic delocalization parameters (in  $\text{pm}^2$ ) of  $C_6H_6$  and  $C_6D_6$  as a function of temperature.  $d_{\text{tot}}^2$  abbreviates the overall delocalization including thermal ( $d_c^2$ ) and quantum ( $d_q^2$ ) degrees of freedom. The difference between the  $d_{\text{tot}}^2$  and  $d_q^2$  curves measures the classical thermal atomic delocalization  $d_c^2$ . In the schematical display this difference is feasible only in the harmonic oscillator approximation. The curves labeled with square and circular symbols have been derived via PIMC simulations in a  $T$  mesh of 50 K. All other curves are based on the harmonic approximation. For further details see the inlaid definitions.

in the atomic delocalization of H and D are immediately seen. The  $T = 0$  K quantum delocalization  $d_q^2$  of the H atoms amounts to roughly  $370 \text{ pm}^2$ . It is reduced to roughly  $250 \text{ pm}^2$  for the deuterium atoms. Both  $d_q^2$  values at  $T = 0$  K have been derived in the ho approximation. The two  $T = 0$  K values of  $d_q^2$  imply zero-point amplitudes of H and D of roughly  $19.2$  and  $15.8 \text{ pm}$ . With decreasing temperature the  $d_q^2$  curves calculated in the PIMC formalism and in the harmonic model start to deviate. The zero-point fluctuations are underestimated by the ho approximation. With increasing temperature  $d_{\text{tot}}^2$  is enhanced while  $d_q^2$  is a decreasing function of  $T$ . This behaviour reflects the continuous transition from a regime with quantum tunneling to a regime of thermal fluctuations. The  $d_{\text{tot}}^2$  and  $d_q^2$  curves of H and D indicate that  $C_6H_6$  and  $C_6D_6$  differ in the relative importance of quantum effects to the net spatial delocalization of the non-carbon nuclei. Let us consider the room temperature (RT) behaviour of the H and D atoms. In  $C_6D_6$  the thermal delocalization  $d_c^2$  is of the same order of magnitude as the quantum effect  $d_q^2$  (ho approximation). In  $C_6H_6$  roughly 75 % of the atomic delocalization is

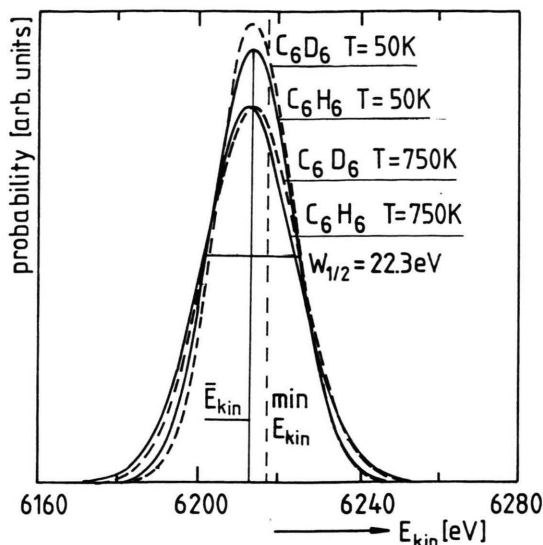


Fig. 2. Distribution function of the *ab initio* (3-21 G basis set) based electronic kinetic energy  $E_{\text{kin}}$  of  $\text{C}_6\text{H}_6$  and  $\text{C}_6\text{D}_6$  at 50 and 750 K. The broken vertical line symbolizes  $E_{\text{kin}}$  derived for the single-configuration calculation (min), and the full vertical line denotes  $\bar{E}_{\text{kin}}$  of  $\text{C}_6\text{H}_6$  at 50 K. All values in eV.

due to quantum processes. The larger atomic mass of the carbons leads to a strong attenuation of the corresponding atomic delocalization. But note that the squared zero-point amplitude of C amounts to roughly  $95 \text{ pm}^2$  which corresponds to a spatial uncertainty of  $9.75 \text{ pm}$ . The results portrayed in Fig. 1 indicate that quantum effects at RT are non-negligible even for the carbon atoms.

In the following we discuss the influence of these large spatial nuclear degrees of freedom on electronic expectation values. In Table 1 we relate the single-configuration values  $E_i$  of the electronic Hamiltonian to the corresponding ensemble averages  $\bar{E}_i^*$ . Let us start with the discussion of the kinetic energy of the electrons  $E_{\text{kin}}$  and  $\bar{E}_{\text{kin}}^*$ . The *ab initio* data in Table 1 show that the spatial delocalization of the  $\text{C}_6\text{H}_6$  nuclei leads to a reduction in the electronic kinetic energy of  $4.116 \text{ eV}$  ( $\text{C}_6\text{H}_6$ ,  $T = 50 \text{ K}$ ). We wish to reemphasize that such an effect is accessible in an all-quantum description of fermion systems, but remains unconsidered in the conventional methods of electronic structure theory. At  $750 \text{ K}$  the kinetic energy of the  $\text{C}_6\text{H}_6$  electrons is lowered by additional  $0.906 \text{ eV}$  (reference:  $T = 50 \text{ K}$ ). The  $T = 50$  and  $750 \text{ K}$  values of  $\bar{E}_{\text{kin}}^*$  indicate the dominating influence of zero-point effects; thermal corrections to the ensemble

quantities are of minor importance only. Substitution of H against D leads to a less pronounced reduction in the electronic kinetic energy, i.e. computational errors of an electronic structure approach in a frozen core approximation are smaller in  $\text{C}_6\text{D}_6$  than in  $\text{C}_6\text{H}_6$ . The  $T = 50 \text{ K}$  value of  $\bar{E}_{\text{kin}}$  of  $\text{C}_6\text{D}_6$  amounts to  $3.527 \text{ eV}$  while the high-temperature shift in the electronic kinetic energy amounts to  $4.416 \text{ eV}$  into the direction of smaller energies. Next we consider the distribution functions of  $E_{\text{kin}}$  which lead to the ensemble averaged quantities  $\bar{E}_{\text{kin}}$  and  $\bar{E}_{\text{kin}}^*$ . In Fig. 2 we have portrayed the distribution functions of  $E_{\text{kin}}$  of  $\text{C}_6\text{H}_6$  and  $\text{C}_6\text{D}_6$  at 50 and  $750 \text{ K}$ . The width at half maximum  $W_{1/2}$  of the four distribution functions exceeds  $22 \text{ eV}$ , an indicator of the strong shifts of the electronic kinetic energy as a function of the nuclear spatial degrees of freedom of the quantum and thermal type. Possible consequences of the ensemble averaging for electronic momentum properties are as follows. As already mentioned and as shown in Fig. 2, the nuclear spatial degrees of freedom reduce the electronic kinetic energy;  $\bar{E}_{\text{kin}}$  is predicted below  $E_{\text{kin}}$ . This inequality indicates that smaller electronic momenta become of higher probability under the influence of the nuclear dynamics. Unfortunately it is not trivial to transfer this all-quantum result for  $\bar{E}_{\text{kin}}$  to calculated Compton profiles or reciprocal form factors. These quantities correspond to a superposition of different one-electron contributions which may have a rather complex analytical shape as a function of the momentum coordinate. We tentatively assume that momentum properties calculated within a single-configurational approach should show the largest errors in the region of smaller momenta.

The PIMC results in Table 1 show that the ensemble shifts calculated for the two-electron and core-core repulsions ( $E_{\text{el}}$ ,  $E_{\text{nuc}}$ ) and for the electron-core attraction ( $E_{\text{el-nuc}}$ ) are even much larger than the shifts predicted for  $E_{\text{kin}}$ . The spatial uncertainty of the  $\text{C}_6\text{H}_6$  nuclei causes a reduction in  $E_{\text{el}}$  of  $28.487 \text{ eV}$  ( $T = 50 \text{ K}$ );  $E_{\text{nuc}}$  is reduced by  $27.449 \text{ eV}$ . We recognize that all elements of the electronic Hamiltonian, which measure the energetic costs in the formation of chemical bonds ( $E_{\text{kin}}$ ,  $E_{\text{el}}$ ,  $E_{\text{nuc}}$ ) are reduced under the influence of the spatial fluctuations of the nuclei. These ensemble shifts are easy to explain. The nuclear dynamics causes a net increase of all interatomic separations. This effect is enhanced with increasing anharmonicities in the interatomic interaction. The attenuation of the two Coulomb repulsion terms  $E_{\text{el}}$  and  $E_{\text{nuc}}$  is the straightforward response

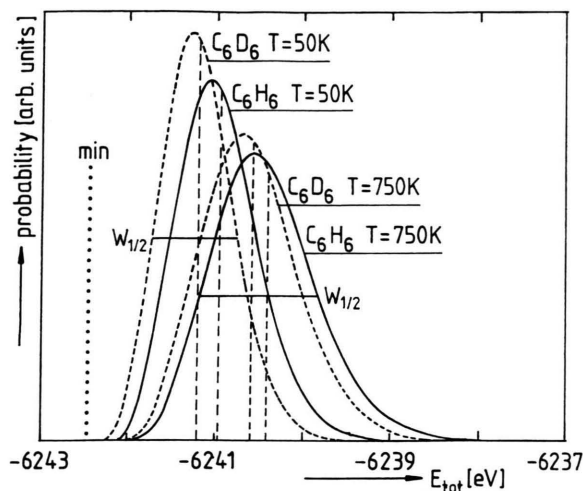


Fig. 3. Distribution function of the *ab initio* total electronic energy  $E_{\text{tot}}$  of  $\text{C}_6\text{H}_6$  and  $\text{C}_6\text{D}_6$  at 50 and 750 K. The dotted vertical line symbolizes  $E_{\text{tot}}$  derived for the single-configuration approach (min) and the broken lines denote the ensemble averages  $\bar{E}_{\text{tot}}$ . All values in eV.

to the nuclear quantum and thermal delocalization. But note that these atomic fluctuations have a second energetic consequence. They enhance the size of the volume elements accessible to interatomic electron delocalization (= electronic sharing). It is this enhanced spatial uncertainty of the electrons which implies a reduced momentum uncertainty and thus a reduction of the kinetic energy of the electrons. The all-quantum results summarized in the table, however, indicate that these three stabilizing  $\bar{E}_i^*$  elements ( $i = \text{kin}, \text{el}, \text{nuc}$ ) are overcompensated by the raise in the electron-core attraction  $\bar{E}_{\text{el-nuc}}$  under the influence of the nuclear dynamics. The ensemble averaged Coulomb attraction is 61.610 eV above the corresponding single-configuration number. Note that  $\bar{E}_{\text{el-nuc}}$  is of negative sign. The combined influence of the three energy increments of the potential energy of the electrons yields a destabilizing ensemble shift of 5.674 eV ( $\text{C}_6\text{H}_6$ ,  $T = 50$  K).  $\bar{E}_{\text{kin}}^*$  and  $\bar{E}_{\text{pot}}^*$  act into opposite directions. The ratio  $\bar{E}_{\text{pot}}^*/\bar{E}_{\text{kin}}^*$  differs strongly from the “equilibrium virial coefficient” of  $-2$ . In  $\bar{E}_{\text{tot}}^*$ , the energetic shift parameters  $\bar{E}_{\text{pot}}^*$  and  $\bar{E}_{\text{kin}}^*$  compensate each other to a large extend. The (rather small)  $\bar{E}_{\text{tot}}^*$  value of 1.558 eV ( $\text{C}_6\text{H}_6$ ,  $T = 50$  K) is an outcome of ensemble corrections to electronic expectation values which are large in magnitude but differ in sign.

The distribution functions of  $E_{\text{tot}}$  are visualized in Figure 3. The discussed compensation of large numbers restricts the  $W_{1/2}$  parameters to a rather narrow interval. In the schematical diagram we find  $W_{1/2}$  elements between 1.00 eV ( $\text{C}_6\text{D}_6$ ,  $T = 50$  K) and 1.44 eV ( $\text{C}_6\text{H}_6$ ,  $T = 750$  K). Remember that  $\bar{E}_{\text{tot}}^*$  has to be identified with the potential energy  $V$  of the nuclear problem. In the harmonic approximation ( $V = T'$ ) the  $\bar{E}_{\text{tot}}^*$  numbers in the table can be equated with the kinetic energy of the nuclei  $T'$ . This means that the calculated ensemble shifts in the kinetic energy of the electrons exceed the kinetic energy of the nuclei by a factor of almost 3. Note that  $T'$  and  $\bar{E}_{\text{kin}}^*$  act into opposite directions. The detailed analysis of the *ab initio* results has demonstrated that the ensemble shifts of the electronic kinetic energy are caused exclusively by the valence electrons of the compounds studied. It is self-explanatory that this valence electronic effect in the kinetic energy, which has been neglected in all calculations of electronic momentum properties reported up to now, is of much larger importance than the neglect of the nuclear kinetic energy. Remember that contributions from quantum particles to Compton profiles and other momentum properties are enhanced with increasing real-space extension of the corresponding wave function (i. e. electronic versus nuclear wave function).

We expect that the error sources in the calculation of Compton profiles, which have been discussed in the literature, should be smaller than the errors caused by the neglect of ensemble effects in the determination of the electronic kinetic energy. The  $\bar{E}_{\text{kin}}^*$  numbers quoted in Table 1 are of the same order of magnitude as C-C, C-H or C-D binding energies. To reemphasize; conventional electronic structure calculations yield  $E_{\text{kin}}$  as well as the underlying single-configuration momentum densities.  $\bar{E}_{\text{kin}}$  or  $\bar{E}_{\text{kin}}^*$  and ensemble averaged momentum densities are accessible only via all-quantum simulations where the spatial degrees of freedom of the nuclei are taken into account in the evaluation of electronic expectation values. The PIMC results summarized in the table indicate a here called “electronic” isotope effect. We have adopted this descriptor to characterize isotope effects in bare electronic expectation values. The difference between the ensemble averaged  $\bar{E}_{\text{kin}}^*$  parameters of  $\text{C}_6\text{H}_6$  and  $\text{C}_6\text{D}_6$  at  $T = 50$  K amounts to 0.589 eV. We wish to point out that the ensemble shifts caused by quantum tunneling and isotope effects in the corresponding  $\bar{E}_i^*$  elements are attenuated with increasing mass of the

atomic nuclei. Isotope effects correspond to a maximum, when H is replaced by D. It is beyond our experience to decide whether or not isotope shifts as encountered in Table 1 can be detected experimentally in measured momentum properties such as Compton profiles.

#### 4. Resumé

The physical consequences of the present theoretical study can be summarized as follows. It has been mentioned above that Compton spectra are dominated by valence electrons. In contrast to diffraction measurements, Compton scattering is very successful in investigations of compounds with light atoms. The present all-quantum study, however, has shown that the limitations of electronic structure calculations of the single-configuration type are particularly strong

for these systems. In the corresponding compounds nuclear quantum effects are of large importance. On the basis of our recent computational experience we assume that improved calculations of Compton profiles or other electronic momentum properties require an all-quantum description as suggested in the present work. But we have to point out that such a proceeding is rather time-consuming. In order to derive the present theoretical results, 24000 *ab initio* calculations of  $C_6H_6$  and  $C_6D_6$  have been performed.

#### Acknowledgements

The present work has been supported by the Fonds der Chemischen Industrie (MCB) and CICYT under contract no. PB 96 - 0874 (RR). We are grateful to G. Wolf for the preparation of the figures and to S. Philipp for critically reading the manuscript.

- [1] R.H. Stuever, *The Compton Effect: Turning Point in Physics*, Science History Publications, New York 1975.
- [2] *Compton Scattering. The Investigation of Electron Momentum Distributions*, B. Williams (ed.), McGraw-Hill, New York 1977.
- [3] T. Asthalter and W. Weyrich, *Z. Naturforsch.* **48a**, 303 (1993).
- [4] P. Kaijser and V.H. Smith, Jr., *Adv. Quantum Chem.* **10**, 37 (1977).
- [5] T. Asthalter and W. Weyrich, *Ber. Bunsenges. Phys. Chem.* **96**, 1747 (1992).
- [6] T. Asthalter and W. Weyrich, *Ber. Bunsenges. Phys. Chem.* **101**, 11 (1997).
- [7] W.A. Reed, *Phys. Rev.* **B18**, 1986 (1978).
- [8] R. Dovesi, C. Ermondi, E. Ferrero, C. Pisani, and C. Roetti, *Phys. Rev.* **B29**, 3591 (1984).
- [9] W. Weyrich, *Ber. Bunsenges. Phys. Chem.* **79**, 1085 (1975).
- [10] R. Ramírez, J. Schulte, and M. C. Böhm, *Chem. Phys. Lett.* **275**, 377 (1997).
- [11] M. C. Böhm, R. Ramírez, and J. Schulte, *Chem. Phys.*, in press.
- [12] J. Schütt, M. C. Böhm, and R. Ramírez, *Chem. Phys. Lett.* **248**, 379 (1996).
- [13] M. Born and J.R. Oppenheimer, *Ann. Phys.* **84**, 457 (1927).
- [14] R.P. Feynman and A.R. Hibbs, *Quantum Mechanics and Path Integrals*, McGraw Hill, New York 1965.
- [15] R.P. Feynman, *Statistical Mechanics*, Benjamin, New York 1972.
- [16] M.J. Gillan, *Phil. Mag.* **A58**, 257 (1988).
- [17] M.J. Gillan, in: *Computer Modelling of Fluids, Polymers and Solids*, C.R.A. Catlow, S.C. Parker, and M.P. Allen (eds.), Kluwer, Dordrecht 1990, p. 155.
- [18] H. Kleinert, *Pfadintegrale*, Wissenschaftsverlag, Mannheim 1993.
- [19] N. Karasawa, S. Dasgupta, and W.A. Goddard III, *J. Phys. Chem.* **95**, 2260 (1990).
- [20] G. Herzberg, *Electronic Spectra of Polyatomic Molecules*, Van Nostrand, New York 1966.
- [21] M.W. Schmidt, K.K. Baldridge, J.A. Boatz, S.T. Elbert, M.S. Gordon, J.H. Jensen, S. Koseki, N. Matsunaga, K.A. Nguyen, J. Su, T.L. Windus, M. Dupuis, and J.A. Montgomery, *J. Comput. Chem.* **14**, 1347 (1993).
- [22] R. Ramírez and M. C. Böhm, *J. Phys.: Condens. Mat.* **14**, 1347 (1995).
- [23] M. C. Böhm and R. Ramírez, *J. Phys. Chem.* **99**, 12401 (1995).
- [24] N. Metropolis, A.W. Rosenbluth, M.N. Rosenbluth, A.H. Teller, and E. Teller, *J. Chem. Phys.* **21**, 10 (1953).
- [25] L. Goodman, A.G. Ozkabak, and S.N. Thakur, *J. Phys. Chem.* **95**, 9044 (1991).
- [26] J. Schulte, M. C. Böhm, and R. Ramírez, *Mol. Phys.*, in press.